Long-gauge fibre optic sensors: performance comparison and applications

Carlos Rodrigues*

LABEST, Faculty of Engineering,
University of Porto,
Rua Dr. Roberto Frias, s/n. 4200-465 Porto, Portugal
E-mail: cfr@fe.up.pt
*Corresponding author

Daniele Inaudi

SMARTEC, Manno, Switzerland/Roctest, St. Lambert, Canada
Via Pobiette 1. CH-6928 Manno, Switzerland
E-mail: inaudi@smartec.ch

Branko Glišić

Princeton University,
E330, EQuad. Princeton, NJ 08544, USA
E-mail: bglisic@princeton.edu

Abstract: Long-gauge deformation sensors have opened new possibilities for the health monitoring of civil engineering structures. They are particularly suitable for applications in structures built of inhomogeneous materials, such as concrete, and with complex strain fields, such as bridges, buildings, dams, whenever the global structural behaviour assessment is of the interest. Different technologies and measurement principles have been developed for measuring average strains over measurement bases that can reach tens of meters with resolutions in the micrometer range. In this work, the performances of seven commercially available alternative solutions, based on fibre Bragg-grating, Fabry-Perot interferometry, stimulated Brillouin scattering, low-coherence interferometry and traditional vibrating-wire technology, were tested and directly compared both in laboratory and in field conditions. The results are presented and discussed, aiming at the assessment of the main characteristics of each technology, and taking into account the principal requirements of in-field civil engineering applications. The efficiency of a monitoring method based on long-gauge sensors is illustrated through an application at the Ricciolo Viaduct in Switzerland.

Keywords: structural health monitoring; SHM; fibre optic sensors; FOS; FOS applications; long-gauge deformation sensors; performance comparison; characteristics assessment; fibre Bragg-grating; FBG; low-coherence interferometry; Fabry-Perot interferometry; stimulated Brillouin backscattering; vibrating-wire.

Reference to this paper should be made as follows: Rodrigues, C., Inaudi, D. and Glišić, B. (xxxx) 'Long-gauge fibre optic sensors: performance comparison and applications', *Int. J. Lifecycle Performance Engineering*, Vol. X, No. Y, pp.000–000.

Biographical notes: Carlos Rodrigues is a PhD student in Civil Engineering at Faculty of Engineering of University of Porto (FEUP), Portugal. Since 2006, he has developed his scientific activity at the Laboratory for the Concrete Technology and Structural Behaviour in the Civil Engineering Department of FEUP. The main subjects of his research activity have been the innovative instrumentation for the structural health monitoring of civil infrastructures, with main focus on the fibre optic sensing solutions, and the structural analysis aiming at the data monitoring interpretation. He has been involved in various projects related to new sensors development, load tests, and short and long-term structural health monitoring.

Daniele Inaudi received a degree in physics at the Swiss Federal Institute of Technology in Zurich (ETHZ) where his graduation work was prized with the ETHZ medal. In 1997, he obtained his PhD in Civil Engineering at the Laboratory of Stress Analysis (IMAC) of the Swiss Federal Institute of Technology in Lausanne for his work on the development of a fibre optic deformation sensing system for civil engineering structural monitoring. In 2005, he received his Master in Business Administration from the University of Southern Switzerland. He is Co-founder and CTO of SMARTEC SA and CTO of Roctest. He is fellow and member of the executive committee of ISHMII and active member of IABMAS, OSA, SPIE, IABSE and fib. He is the author of more than 200 papers, five book chapters, a book on *Fiber Optic Methods for Structural Health Monitoring* and editor of a book on *Optical Nondestructive Testing*.

Branko Glišić received his degrees in Civil Engineering and Theoretical Mathematics at University of Belgrade, Serbia, and PhD at the Swiss Federal Institute of Technology, Lausanne (EPFL), Switzerland. His thesis focuses on the development of fibre optic sensors for particular applications, and auscultation and characterisation of concrete at very early age. He was employed at SMARTEC SA, Switzerland, as a Solutions and Services Manager (2000–2008) where he was involved at different levels of responsibility in numerous structural health monitoring (SHM) projects, EU funded projects and internal R&D projects. Since 2009, he has been employed as an Assistant Professor at Department of Civil and Environmental Engineering of Princeton University. His main areas of interest are structural health monitoring (SHM), fibre optic sensors (FOS) and advanced sensory systems, smart structures and intelligent infrastructure, and sustainable engineering. He is the author of a book entitled *Fibre Optic Methods for Structural Health Monitoring*.

1 Introduction

A structural health monitoring (SHM) system should be able to measure and record the most significant parameters relevant to the structural behaviour aiming at a reliable assessment of the structural condition and damage detection. Identification of the most indicative parameters to monitor, determination of the location of the measurement points, and selection of the SHM systems are significant aspects to consider when aiming to an efficient investment in the design of a monitoring system.

The strains and the deformations are among the most significant and consequently the most required parameters to be monitored in relation to the assessment of the structural behaviour. Strain and deformation monitoring has proved to be able to provide important information about the structural behaviour and to be effective in damage detection. Axial,

bending and shear forces, as well as deformed shapes of the structure under external forces and environmental conditions can be estimated based on monitoring results collected using proper combinations of deformation sensors placed in key locations of the structure (Glisic and Inaudi, 2007). Therefore, many efforts have been made by researchers and companies to find more accurate, economic, easy to install, and reliable measurement systems (e.g., SHMII, 2009).

Different methodologies, technologies and functional principles have been developed with successful results. Several fibre optic sensing technologies have reached market maturity and are employed in routine SHM applications worldwide. In order to assess the performance of several different fibre optic sensors (FOS) technologies and to evaluate their suitability for civil engineering applications, comparisons between various fibre optic long-gauge solutions and conventional sensing solutions were performed in laboratory and in field conditions. This work focuses on the most utilised fibre optic long-gauge deformation technologies at industrial and commercial level. The comparison points to a better characterisation of the current state-of-the-art in the FOS market. The accuracy, precision, and temperature sensitivity were assessed and directly compared, focusing on the specific needs of civil engineering applications. As an example of a field application of long-gauge FOS, a practical application to the assessment of a curved Viaduct in Switzerland is given at the end of the article.

2 Long-gauge deformation sensors

2.1 Introduction

With reference to their spatial disposition, sensors are classified as discrete or point sensors or as continuous or distributed sensors. A point sensor measures a parameter related to a single position in the structure, whereas distributed sensors measure the parameter at several positions and can replace a chain of point sensors.

Point sensors designed to measure relative displacement or average strain between two predefined points of a structure are called deformation sensors. The distance between these two points is called the gauge length of the sensor. With respect to the gauge length, the sensors are conventionally classified in two groups: short-gauge and long-gauge sensors. Traditional sensors, such as strain gauges and vibrating wires, belong to the group of short-gauge sensors. Depending on their type and packaging, optical-fibre sensors can function as short-gauge or as long-gauge sensors.

The availability of long-gauge FOS has opened new and interesting possibilities for structural monitoring. Long-gauge sensors allow the measurement of deformations over measurement bases that can reach tens of meters with resolutions in the micrometer range. The long-gauge sensor theory can also be applied to distributed sensing systems (see Subsection 2.2).

Using long-gauge sensors, it is possible to cover the whole volume of a structure with sensors, therefore enabling a global monitoring of it. This constitutes a fundamental departure from standard practice, which is based on the choice of a reduced number of sampling points supposed to be representative of the whole structural behaviour and their instrumentation with short-gauge sensors. This common approach will give interesting information on the local behaviour of the construction materials, but might miss behaviours and degradations that occur at locations that are not instrumented. On the

contrary, long-gauge sensors allow the monitoring of a structure as a whole, so that any phenomenon that has an impact on the global structural behaviour is detected and quantified. In general, short-gauge sensors are more appropriate to study local material properties, while long-gauge sensors are ideal to monitor the global structural behaviour. In order to illustrate this statement, an on-site application is presented in Section 5. Basic notions concerning the gauge length of discrete deformation sensors and its equivalent for the distributed sensors (called spatial resolution) is given in the next section.

2.2 Long-gauge measurement principle

Frequently used construction materials, and notably concrete, can be affected by local defects, such as cracks, air pockets and inclusions. All these defects introduce discontinuities in the mechanical material properties at a meso-level. More indicative for structural behaviour, however, are material properties at the macro-level. For example, reinforced concrete structures are mainly modelled and analysed as built of a homogenous material – cracked reinforced concrete. Therefore, for structural monitoring purposes it is necessary to use sensors that are insensitive to material discontinuities at the micro- and meso-levels.

In inhomogeneous materials, the gauge length of a deformation sensor can cross several discontinuities that influence the measurement and its interpretation. A description of the measurements performed by a deformation sensor is presented in Figure 1 and equation (1) (Glisic and Inaudi, 2007).

Figure 1 Schematic representation of a long-gauge sensor in an inhomogeneous material

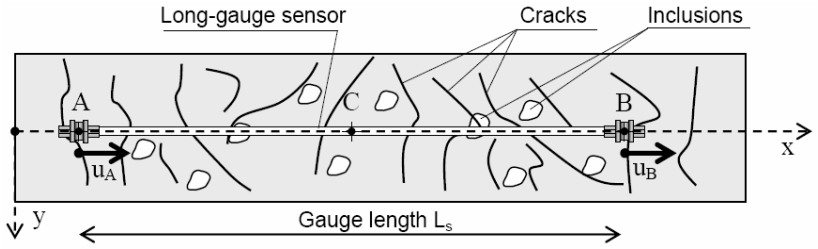

If *A* and *B* are the sensor anchoring points as shown in Figure 1, then the measurement of the sensor represents a relative displacement between them. The measurement of the sensor is then expressed as follows:

$$\varepsilon_{C,s} = \frac{\Delta L_s}{L_s} = \frac{u_B - u_A}{x_B - x_A} = \frac{1}{L_s}\int_{x_A}^{x_B} \varepsilon_{x,s}(x)\mathrm{d}x + \frac{1}{L_s}\sum_i \Delta w_{d,i} \tag{1}$$

where

A, B points delimiting gauge length of the sensor with coordinates x_A and x_B

C midpoint of the sensor with coordinate $x_C = (x_A + x_B) / 2$

$L_s = x_B - x_A$ gauge length at reference time, before the deformation is applied

u_A, u_B	x-axis component of displacements of points A and B after deformation is applied
$\varepsilon_{C,s}$	average strain in point C measured by sensor
$\varepsilon_{x,s}(x)$	strain distribution along the x-axis of the sensor
$\Delta w_{d,I}$	dimensional change of i^{th} ($x_i \in [x_A, x_B]$) discontinuity (crack opening, inclusion dimensional change, etc.) in direction of x-axis, after the deformation is applied.

A short-gauge deformation sensor has a gauge length shorter than the distance between two discontinuities or comparable to the dimensions of the inclusions in the material monitored. Therefore, the measurement performed with short-gauge sensors is strongly influenced by local defects; it provides information related to local material properties and is not suitable for global structural monitoring since global performance cannot be extrapolated from a small number of local observations.

A long-gauge deformation sensor is by definition a sensor with a gauge-length several times longer than the maximal distance between discontinuities or the maximal diameter of inclusions in a monitored material. For example, in the case of cracked reinforced concrete, the gauge length of a long-gauge sensor is to be several times longer than both the maximum distance between cracks and the diameter of inclusions. The main advantage of this measurement is in its nature: since it is obtained by averaging the strain over long measurement basis, it is not influenced by individual local material discontinuities and inclusions, but only by their impact on the global behaviour. Thus, the measurement contains information related to global structural behaviour rather than the local material behaviour.

Distributed fibre-optic sensing presents unique features that have no match in conventional sensing techniques. The ability to measure the strain at thousands of points along a single fibre is particularly interesting for the monitoring of large structures, such as bridges, pipelines, flow lines, oil wells, dams and dykes.

Although distributed sensors are sensitive to strain at every point along the sensing optical fibre, they measure at discrete points that are spaced by a constant value, called the sampling interval, and the measured parameter is actually an average strain measured over a certain length, called the spatial resolution. The explanation of distributed sensor measurement is presented in Figure 2.

Let us consider a distributed sensor with a total length L_D measured with a sampling interval of L_{SI} and a spatial resolution L_{SR}, as presented in Figure 2. Let x be the coordinate along the distributed sensor, $n = integer(L_D/L_{SI})$, x_0 is the coordinate of the first point on the sensor and $x_i = x_0 + iL_{SI}$, $i = 1, 2, 3,\ldots,n$, are coordinates of the points defined by the sampling interval; see Figure 2(a).

For each point with coordinate x_i the strain is averaged over the segment $[x_i, x_i + L_{SR}]$ as presented in Figure 2(b) to 2(d), and the value of the measurement is attributed to the point xi as presented in Figure 2(e).

Finally, the strain diagram of the measurement obtained is shifted horizontally by L_{SR} / 2, as presented in Figure 2(f), in order to attribute the average strain measurements to the middle point of the averaging segment.

Figure 2 Explanation of distributed sensor measurement

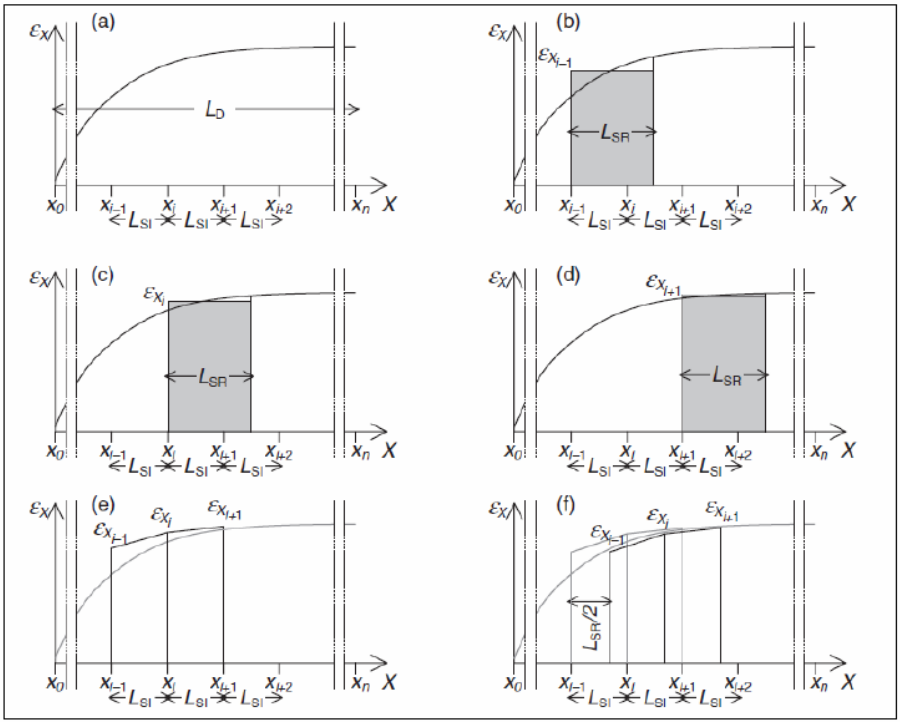

Source: Glisic and Inaudi (2007).

The above discussion supports the statement that distributed measurement performed using a distributed sensor with length L_D and sampling interval L_{SI} provides for the same information as n discrete (point) sensors ($n = integer(L_D/L_{SI})$) with a gauge length of L_{SR}. Since the distributed sensor provides for the same information as the discrete (point) sensors, all the considerations related to notion of gauge length developed earlier are applicable to the notion of spatial resolution of distributed sensors.

This general principle, however, is not valid for abrupt strain changes or concentrated strains (such as those generated by cracks). In this case, the measurement resulting from a distributed sensing system can be unpredictable and possibly lead to measurement errors. Advanced algorithms have been developed to deal with such situations, but exceed the scope of this paper (Ravet et al., 2009). Appropriate sensor designs, allowing for controlled strain redistribution over a length compatible with the spatial distribution, can also be used to minimise these problems.

Based on the discussion presented in this subsection, it is clear that a division between short and long-gauge sensor depends on the properties of the material to be monitored. Measures (2001) proposes the length of 50 mm as the limit between short and long gauge lengths. While this division can be acceptable for homogeneous materials, such as steel, it will not apply for inhomogeneous materials, such as concrete, where the aggregate size can be as big as 32 mm, and the distance between the structural cracks 100 to 200 mm. That is why, for practical purposes, we propose a classification of the

strain sensor as shown in Figure 3, where a unique gauge length limit between short and long gauge sensors is not specified.

Figure 3 Classification of deformation sensors based on their gauge length

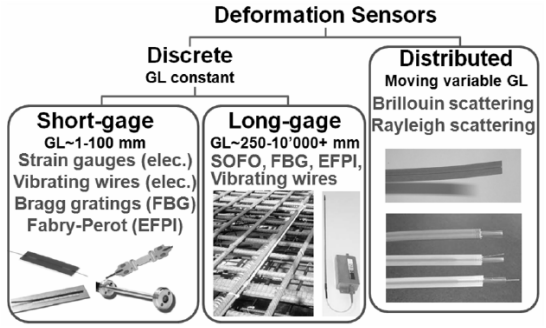

2.3 Long-gauge sensing solutions

The market of monitoring solutions for civil engineering applications offers nowadays a large variety of long-gauge deformation sensors. In this work, seven different available solutions for creating long-gauge sensors were tested, aiming at the assessment of their current performance in civil engineering applications. Most of these solutions are based on fibre optic technologies, using different principles such as fibre Bragg-grating (FBG) (Othonos, 1997; Kersey et al., 1997), low-coherence interferometry (Surveillance d'Ouvrages par Fibres Optiques, SOFO) (Inaudi, 1997; Inaudi et al., 1997), extrinsic Fabry-Perot interferometry (EFPI) (Petuchowski et al., 1981; Yoshino et al., 1982), and stimulated Brillouin scattering (Horiguchi et al., 1989; Nikles et al. 1996). A conventional vibrating-wire sensor (Hornby, 1992) was also included in the tests for comparison between this conventional sensor and the more recent FOS.

Table 1 Long-gauge sensing solutions selected for tests

System	*Sensor*	*Reading unit*	*Measuring principle*	*Supplier*
A	SOFO deformation	SOFO VI	Low coherence interferometric sensor with interferometry readout	Smartec, SA
B	SOFO deformation	MuST Light	Low coherence interferometric sensor with spectral readout	Smartec, SA
C	MuST deformation	MuST Light	Fibre Bragg grating	Smartec, SA
D	FOD displacement	FISO FTI-10	Fabry-Perot	Fiso Technologies
E	Vibrating Wire Jointmeter VW-JM	Campbell AVW200	Vibrating wire (conventional electrical-based sensor)	Roctest
F	SMARTprofile	DiTeSt STA-SMA	Brillouin backscatering	Smartec, SA
G	SMARTape	DiTeSt STA-SMA	Brillouin backscatering	Smartec, SA

Table 1 summarises the long-gauge sensing solutions tested in this work. All the selected solutions are offered at a market maturity level and were developed for applications in civil engineering structures. Each solution is a combination of a long-gauge deformation sensor with a suitable reading unit, defined taking into account the most frequent solutions provided by the different systems suppliers. All sensors were configured to have similar application, being therefore possible alternatives to the same purpose. In this particular case, they were manufactured to be surface mounted with a gauge length of 1.0 m.

2.3.1 SOFO deformation sensor

The *SOFO* system is based on the principle of low-coherence interferometry in FOS (Inaudi et al., 1997). The SOFO sensor, commercialised by SMARTEC, was designed to be easily installed in civil engineering structures and can be used both in embedded and in surface mounted applications with a gauge length that can reach 10 m or more. The long-gauge sensor and the reading unit are presented in Figure 4.

Figure 4 (a) SOFO deformation sensor and (b) SOFO VI reading unit (see online version for colours)

(a) (b)

Figure 5 shows SOFO sensor internal architecture. The sensitive part consists in a pair of optical fibres installed inside a suitable package. One of the two fibres, the measurement fibre, is pre-tensioned and mechanically coupled to the two anchorage points in order to follow the structure's deformations, while the other fibre, the reference fibre, is free of deformation and provides for temperature compensation. The change in the difference of the length of these two fibres corresponds to the change in the integrated strain between the two anchorage points.

Figure 5 Standard SOFO deformation sensor configuration (see online version for colours)

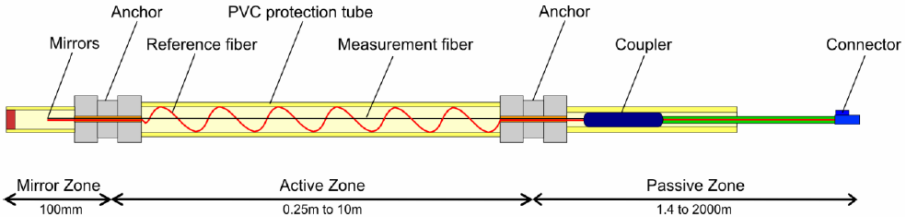

A SOFO reading unit, SOFO VI (see Figure 4), is also commercialised by SMARTEC and measures the length difference between the reference and measurement fibre using a Michelson interferometer. The infrared emission of a super-luminescent LED is launched into a single-mode fibre and sent to the sensor. Then, the light is reflected by the two mirrors silvered at extremities of the measurement and the reference fibre and guided back to a Michelson interferometer in the reading unit. The Michelson interferometer has one arm terminated by a mobile mirror. By moving this mirror, a modulated signal is obtained when the length difference between the fibres in the analyser matches the length difference between the fibres in the sensor (Inaudi, 2000). The specified repeatability of the system is 2 micrometers regardless of the gauge length of the sensor, which corresponds to 2 microstrains (0.002 mm/m) for a sensor with gauge length of 1 m.

An alternative demodulation technique has also been developed based on the analysis of the light spectrum reflected by the interferometric sensor in the frequency domain (Inaudi et al., 2005). This technique is promising because it allows the combination of different fibre optic technologies, such as SOFO and FBG, in the same reading unit, and it is also assessed in this work using the MuST reading unit presented in the next subsection.

2.3.2 MuST deformation sensor

The MuST deformation sensor is similar to the previous SOFO sensor in terms of external package, see Figure 6. The difference resides in the internal components, i.e., the sensing element, and technology in use. The MuST sensor is based on the FBG technology, which uses the wavelength of the light reflected by a grating inscribed in the fibre core as encoding parameter for strain and temperature measurement (Kersey et al., 1997; Othonos, 1997). Strain and temperature changes are linearly correlated to changes in reflected wavelength.

Figure 6 (a) MuST reading unit and (b) MuST deformation sensor (see online version for colours)

(a) (b)

Figure 7 schematises the internal architecture of the MuST deformation sensor. The active part of the MuST deformation sensor is, in this case, composed by only one fibre. This fibre contains an FBG that is pre-tensioned inside the protective pipe and mechanically coupled to the two anchorage points. The deformation of the structure induces a deformation in the measurement fibre that causes a change in the strain and therefore in the reflected wavelength of the FBG. The strain measured in the FBG corresponds directly to the average strain between the two anchorage points, assuming that the strain distribution along the entire fibre is uniform.

The simultaneous sensitivity to both the strain and temperature is intrinsic to the FBG technology. While the effect of temperature is generally negligible in laboratory conditions, where the temperature can be controlled and kept constant, in field applications the temperature can vary significantly and temperature compensation is vital for an accurate measurement of the stain. Therefore, a loose, strain-free FBG is placed near the strain sensing part of the sensor, and it is used for temperature compensation, but also for temperature monitoring.

The MuST reading unit, tuned by MicronOptics (see Figure 7) and distributed by the Roctest Group, is based on a swept wavelength laser light source. Two different versions, MuST light and MuST dynamic, are available for static and dynamic applications, respectively, and MuST light was used for the testing. The specified repeatability of the MuST system with temperature compensation is 2 microstrains (0.002 mm/m).

Figure 7 Standard MuST deformation sensor configuration (see online version for colours)

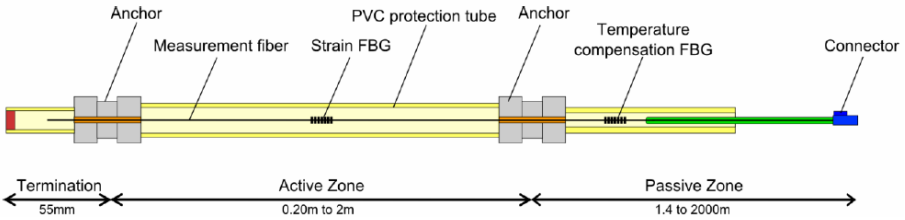

The MuST reading unit was also used as an alternative to read SOFO sensors (see Table 1 and previous subsection). In this case, the full reflected spectrum is analysed in order to extract the spectral modulation frequency introduced by the sensor.

2.3.3 FOD deformation sensor

The FOD sensor is a displacement transducer that is, in terms of packaging, similar to a conventional linear variable differential transformer (LVDT), as illustrated in Figure 8. However, this displacement transducer is based on the EFPI technology (Yoshino et al., 1982; Petuchowski et al., 1981). The FOD is manufactured and commercialised by Roctest. The gauge length is defined by the length of the sliding rod (see Figure 8).

Figure 8 (a) FOD displacement sensor and (b) UMI reading unit (see online version for colours)

(a) (b)

The functional principle of the FOD is based on a thin film Fizeau interferometer device (TFFI) (Duplain et al., 1997) connected to the sliding rod as shown on Figure 9. The TFFI can be seen as a spatially distributed Fabry-Perot cavity where the cavity length

varies along the lateral position. The tip of an optical fibre faces the surface of the TFFI which is moved relative to the optical fibre extremity and causes a variation on the reflected interferometric signal.

Figure 9 FOD sensor configuration

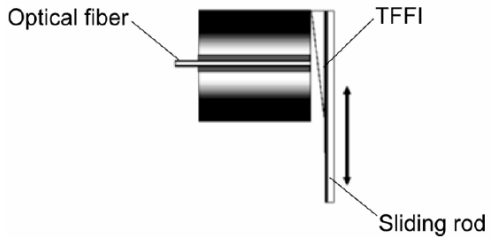

The Roctest Group provides white-light fibre optic reading units for the FOD sensors, and model FTI-10 was selected for testing. Through the use of a white-light cross-correlator, these reading units are capable of measuring with nanometer accuracy the absolute cavity length of Fabry-Perot fibre optic transducers.

While the EFPI sensing element itself is not sensitive to temperature, the sliding rod is subjected to dimensional changes under temperature variations and thus temperature compensation is needed. The specified repeatability of the system is 20 μm.

2.3.4 SMARTape and SMARTprofile

The SMARTape and SMARTprofile are distributed sensors (sensing cables), developed and commercialised by SMARTEC. Both sensors are used for strain sensing based on Brillouin scattering.

The packagings of both sensors are designed to allow a simple and easy installation and a good transfer of the structural strain to the sensing optical fibres. The SMARTape is composed of an optical fibre embedded in a tape of glass-fibre-reinforced thermoplastic as depicted in Figure 10. The SMARTprofile is designed to combine strain and temperature measurements. This sensor consists of two bonded and two free optical fibres embedded into a polyethylene thermoplastic profile as shown in Figure 11. Both can be installed by fusing, gluing or clamping to the structure.

Figure 10 (a) Cross-section and (b) sample of SMARTape sensor (dimensions in mm) (see online version for colours)

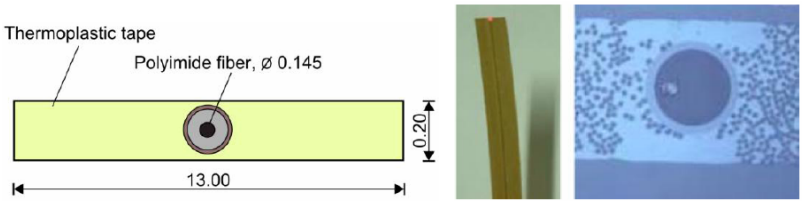

(a) (b)

Figure 11 (a) Cross-section and (b) sample of SMARTprofile sensor (dimensions in mm) (see online version for colours)

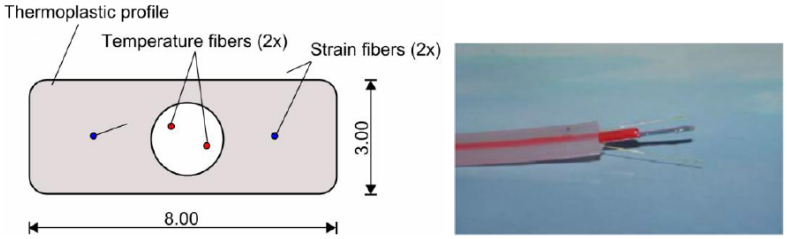

(a) (b)

The encoding parameter for both sensors is the Brillouin frequency of the light scattered back from each point of a single-mode fibre. The change in the Brillouin frequency depends linearly on the changes in strain and temperature (Horiguchi et al., 1989; Nikles et al., 1996). SMARTEC and Omnisens commercialise the reading unit for distributed structural monitoring based on the stimulated Brillouin scattering, named DiTeSt (see Figure 12). The local characteristics of stimulated Brillouin scattering are measured thanks to an innovative and highly reliable configuration developed by the Metrology Laboratory of the Swiss Federal Institute of Technology of Lausanne (Thevenaz et al., 1999). This measurement technique relies on the use of a single laser source and is therefore totally self-referenced allowing periodic measurements without any preliminary calibration. It features a measurement range up to 50 km with a spatial resolution of 0.5 m. In the tests the spatial resolution was set to 0.5 m.

Figure 12 DiTeSt reading unit based on Brillouin backscattering (see online version for colours)

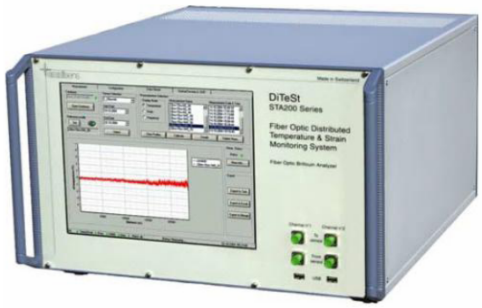

The Brillouin frequency change is sensitive to both strain and temperature, thus temperature compensation is necessary. The specified repeatability of the system is 20 microstrains (0.020 mm/m).

2.3.5 VW-JM sensor

The VW-JM sensor is a vibrating wire jointmeter that is designed to be used to measure displacement at joints and cracks in structures and rock masses. It consists of a vibrating wire displacement transducer inside telescoping stainless steel housing, similar to that

used for FOD sensor (see Figure 13). This jointmeter can be used as long-gauge deformation sensors. A rod defines the gauge length of the sensor, similar to FOD sensor.

Figure 13 (a) VW-JM sensing system based on vibrating wire sensing and (b) AVW200 reading unit (see online version for colours)

(a) (b)

The VW-JM sensor is based on a vibrating wire sensing element linked to a spring at one end and to the rod at the other end. The movement of the rod, pulled from the gauge body, elongates the spring causing an increase in tension which is sensed by the vibrating wire element through a change in its resonance frequency. This change can be measure with a reading unit for vibrating wire sensors.

In the present work, the AVW200 reading unit was selected for automatic measurements. It is a two-channel vibrating wire spectrum analyser module tuned by Campbell Scientific, Inc. The AVW200 measures the resonant frequency of the taut wire in a vibrating wire sensor through Fourier transformation of the response of the wire previously excited. The reading unit automatically excites the wire and analyses the resulting spectrum to determine the wire's resonant frequency.

The vibrating wire sensing element has integrated temperature sensor which is used for temperature compensation. The specified repeatability of the system is 10 μm.

3 Description of testing

3.1 General

The following important characteristics of the presented monitoring systems were tested in the laboratory and on-site:

- accuracy of the monitoring systems
- precision of the monitoring systems
- temperature cross-sensitivity of the reading units
- temperature cross-sensitivity of the sensors.

The performance of the presented systems was directly compared by exposing the sensors to identical strain and temperature conditions. First the laboratory tests were performed in order to assess the accuracy and precision of the sensors, and the temperature cross-sensitivity of the reading units. Then, all the systems were installed in parallel on the Ricciolo Viaduct, in Manno Switzerland, and their performance is compared in real, on-site conditions. Particular attention was paid to the assessment of temperature cross-sensitivity of the sensors, exposed to natural temperature fluctuations.

3.2 Accuracy of measurement

The accuracy of each measurement system was assessed in laboratory, by comparing the closeness of agreement between the measured deformation and the deformation imposed to the respective long-gauge sensor. Potential errors of non-linearity, non-repeatability and hysteresis, of each system including the reading unit and the sensor combined were assessed. A quantitative evaluation was performed through the quantification of the measurement errors.

The test set-up is depicted in Figure 14. It is composed of a highly rigid support with two anchoring pieces where the sensor is fixed. While one anchoring is fixed and connected firmly to the support, the other is movable and allows the imposition of controlled deformations on the sensor by means of a precision translation stage commanded through a micrometer screw. Imposed deformations were measured using certified displacement digimatic indicator with an absolute error of 0.001 mm, which for 1 m gauge length corresponds to an average strain of 1 microstrain (0.001 mm/m). In total 20 increments of 500 microstrains (0.5 mm/m) were applied and measurements were performed after each increment. During the test, the measurements registered with the systems under test and the values registered by the absolute displacement digimatic indicator were compared to assess the slope error and the standard deviation of the residual error.

Figure 14 Test set-up used for the accuracy assessment, (a) schematic illustration of the accuracy test set-up (b) global view of the laboratory set-up (see online version for colours)

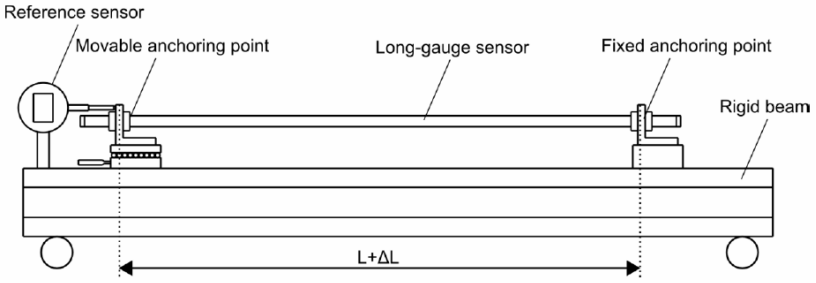

(a)

(b)

3.3 Precision of measurement

The precision of each measurement system was assessed in terms of repeatability, i.e., keeping the same condition of measurement that includes same locations, operators, measuring systems, constant temperature, and constant deformation.

In order to appraise the precision of the different long-gauge sensing systems, the sensor under the test was installed to the set-up previously used for the testing of accuracy. This time both anchoring points were kept fixed after a constant deformation was imposed to the sensor. For each system under test, 100 measurements were carried out and the standard deviation of the obtained results was calculated.

3.4 Temperature cross-sensitivity of the reading units

The cross-sensitivity of the reading units to temperature variations was assessed in a third laboratory test. Although this characteristic is not usually present in the sensing requirements, it has a great importance in field applications where the reading units are exposed to significant temperature variations. Each sensor was fixed to the same set-up used to assess the precision of the systems (see Figure 14), and kept under constant strain and temperature conditions. During the test period, the reading unit was transferred to the interior of a controlled temperature cabinet. The temperature around the reading unit changes from the ambient temperature (22°C) to zero degrees inside the cabinet. After the stabilisation of the temperature of the reading unit, it was removed from the cabinet and put back to the ambient temperature. Measurements were taken during the test period in order to identify potential changes and the dependence of the measurements on the reading unit temperature change.

3.5 Temperature cross-sensitivity of the sensing systems

The temperature cross-sensitivity of complete monitoring systems, including the reading unit and the sensor combined together could not be tested in laboratory due to unavailability of a suitable testing equipment able to contain the long gauge sensors. Not being able to conduct a controlled temperature test, it was decided to test the sensors performance on a real structure subject to natural temperature fluctuations. This was performed on the Ricciolo Viaduct, in Switzerland. This viaduct offers particular structural conditions and installations facilities to carry out the tests.

Figure 15 General views of the long-gauge deformation sensors installed on Ricciolo Viaduct for assessment of their performance in real field conditions (see online version for colours)

For the propose of the testing different sensors were installed at the same location and measured at the same time, which allows a direct and effective comparison of the performance of each system. The parallel installation of the seven sensing systems under

test in a cross-section with suitable characteristics for a comparative study was carried out. An intermediate bridge deck cross-section was selected taking into account the expected less significant effects of bending moments, and a more constant distribution of strain along the height of the cross-section (inflection point).

Temperature sensors were installed next to the deformation sensors and in the concrete. Figure 15 gives an overview of the sensor installation in the bridge with the seven long-gauge sensors installed in the same cross-section. Measurements were taken at 30 minutes intervals during a one-month period.

4 Results

4.1 Accuracy of measurement

For each system under analysis, the measurement errors were assessed correlating the measurements of each system and the imposed deformation. Twenty deformation levels within the range of 1% of elongation were considered. The best linear regression model was calculated, as shown in Figure 16 illustrating the results of SOFO system.

Figure 16 Accuracy test results for System B composed of SOFO sensor and MuST RU based on a low coherence interferometric sensor demodulated in the spectral domain (see online version for colours)

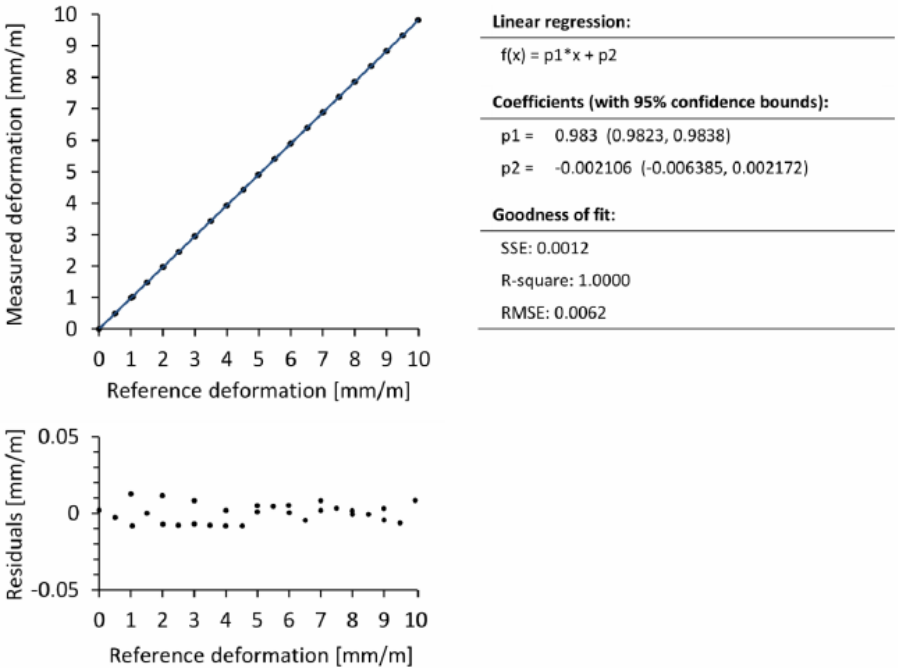

Two indicators were used to compare the measurement errors, namely the slope error given by the difference between the unitary value and the slope achieved with the best linear regression model (p1 in Figure 16), and the root mean square error (RMSE) of the

residuals. The slope error quantifies the deviation of the real value from the measurement obtained by applying the calibration coefficients provided by the manufacturers. The RMSE quantifies the deviation from the best linear fit, being an indicator regarding the sensor linearity, and it can reflect all the random and hysteresis errors. R-square indicator was not used in this comparison since it was for all sensors higher than 0.999. The results achieved for the different systems under test are shown in Figure 17 for comparison.

Figure 17 Comparison of the measurement errors achieved in accuracy tests, (a) slope error (b) RMSE (see online version for colours)

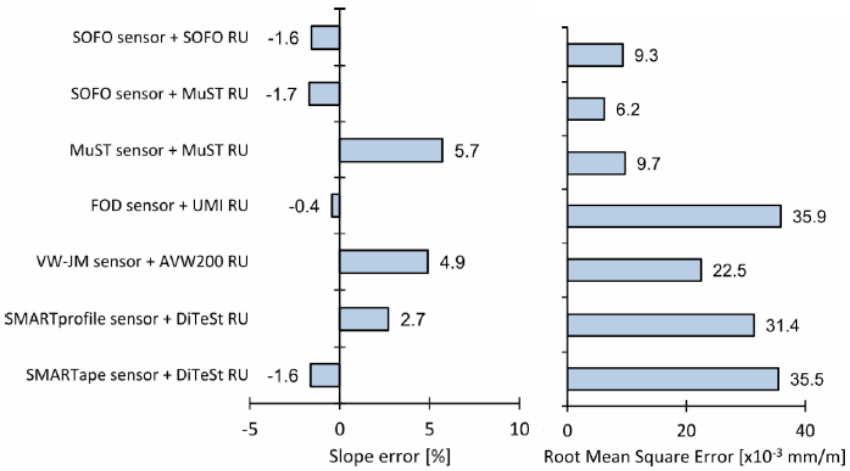

(a) (b)

A maximum slope error by absolute value of 5.7% was achieved when the measurements were adjusted by the best linear regression model. It happened with the MuST system based on an FBG sensor. Although of the MuST system exhibited the greatest error in the fit slope, it was one of the systems with the smallest RMSE. It means that an adjustment in the parameters of the calibration expression used to convert the Bragg wavelength shift to strain can significantly reduce the measurement error of this system. Similar conclusions can be carried out for the other systems.

There was also an excellent agreement between the measurements of the low coherence interferometric sensor, SOFO sensor, with the SOFO VI and MuST reading units demodulated through an interferometric and spectral readout respectively. Moreover, the SOFO sensor when inquired with the MuST reading unit exhibited a better performance, translated by a smaller RMSE. A minimum slope error of 0.4% was achieved for the FOD system (Fabry-Perot inteferometric sensor). In spite of the agreement in slope of the fit model, the RMSE of these sensors was the highest. Some signs of hysteresis were observed in the presented results too. Both distributed sensors exhibited mutually similar performances. The amplitude of the deviations, as well as the RMSE of these two systems was very close.

4.2 Precision of measurement

The standard deviation and the noise amplitude of 100 consecutive measurements (see Figure 18) was used to quantify the repeatability of the various sensing systems. Both characteristics are presented on Figure 19, comparing the performances of the different systems.

Figure 18 Test results referring to repeatability of the system composed of SOFO sensor and SOFO RU based on a low coherence interferometric sensor

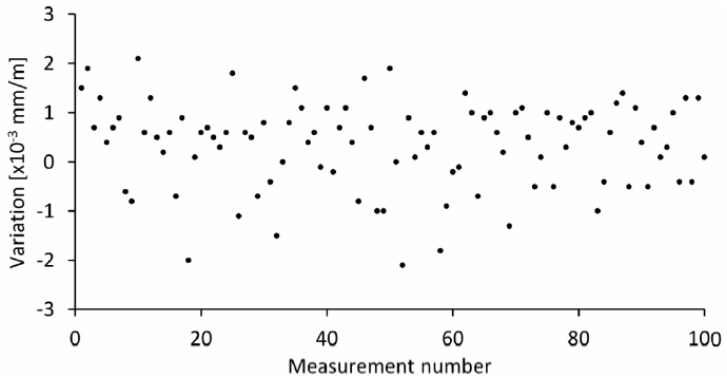

Figure 19 Comparison of the precision of the different system carried out over 10, (a) repeatability (standard deviation) (b) absolute error range (see online version for colours)

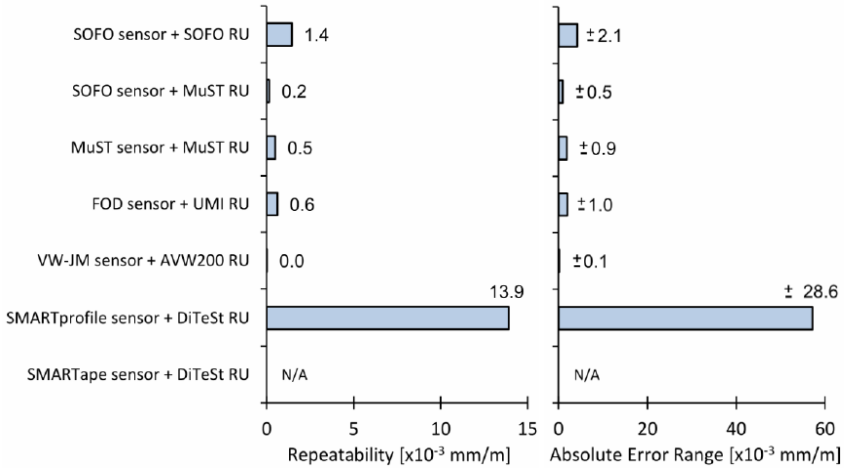

(a) (b)

All the results are contained in the precision limits suggested by the systems suppliers. The conventional vibrating wire-based system exhibited the highest precision. The precision exhibited by this conventional sensor surpasses in about five times the best performance of the fibre optic systems. On the other side, the DiTeSt system, based on a

Brillouin distributed sensing solution, exhibited the lowest precision. The level of precision demonstrated by this system was, as expected, worse than all other systems due to the limitations of the optical technology. It was tested only for the SMARTprofile sensor, since it is not expected that this parameter is sensor-dependant.

It is to highlight that the use of the spectral MuST reading unit with the SOFO sensor, alternatively to the SOFO reading unit, showed a great improvement in the system precision. In this case, the precision increased almost ten times when the interferometric readout is replaced by a spectral one.

4.3 Temperature cross-sensitivity of the reading units

The temperature cross-sensitivity of the reading units was quantified by the standard deviation of the measurement carried out on sensors in constant conditions while the reading unit is subjected to temperature variation. Thus, it is an indicator about the measurement error concerning the cross-sensitivity of the reading units to rapid temperature variations.

Figure 20 shows the root mean square of the results when a temperature variation was induced with the introduction and removal of the reading unit to/from the climatic chamber corresponding to a temperature variation of ±22°C. No significant perturbations due to temperature variations were observed during the tests, and the achieved standard deviations are comparable with the limits of precision prescribed for these reading units and with the tests at constant reading unit temperature.

Figure 20 Comparison of the temperature sensitivity of the reading units under test (see online version for colours)

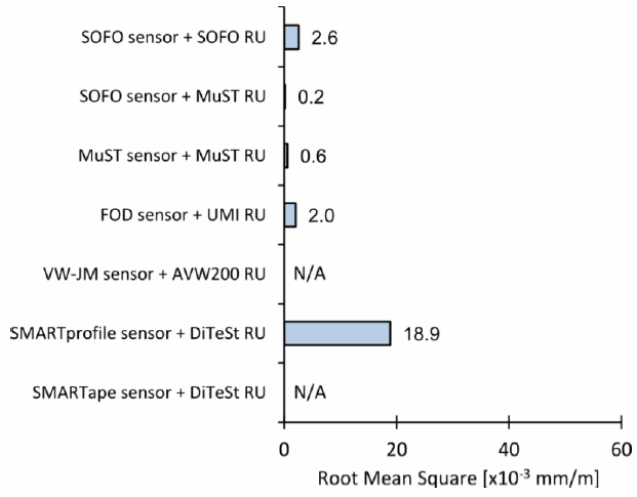

4.4 Temperature cross-sensitivity of the sensing systems

Temperature cross-sensitivity of combined reading units and sensors was derived from the field tests performed on the Ricciolo Viaduct. The SOFO sensor read by the SOFO VI

reading unit is known to be practically insensitive to temperature variations from previous tests (Lienhart, 2005) and it was used as reference to calculate the temperature sensitivity of the other systems. Therefore, a residual thermal strain term was calculated for other sensors by subtracting the measurements of the SOFO sensor from the measurements of the other sensors without any type of temperature compensation. The ambient and concrete temperature was measured aimed at the quantification of the temperature influence on each sensor. The correlation between the measured temperature and the residual thermal strain characterises the temperature cross-sensitivity of each system. Figure 21 shows the correlation between the temperature and the residual thermal strain achieved with the MuST system. Analogous results were obtained for the other systems being compared in Figure 22.

Figure 21 Correlation between the temperature and the residual thermal strain achieved with the MuST system installed on Ricciolo Viaduct (see online version for colours)

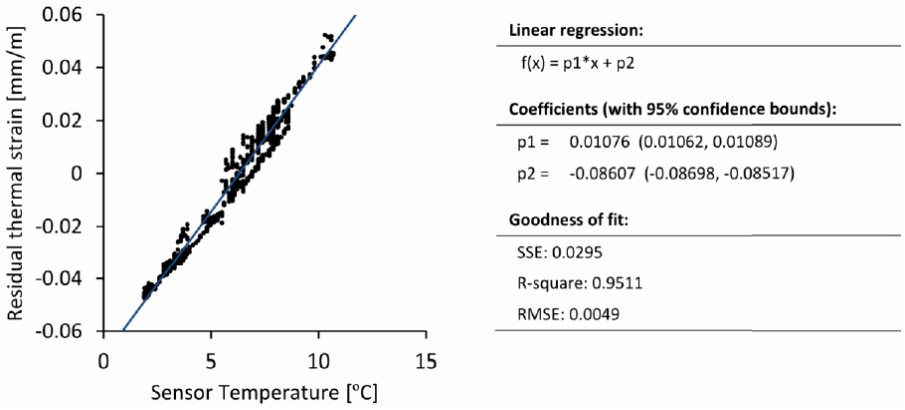

Figure 22 Comparison of the temperature sensitivity exhibited by the various measuring systems on Ricciolo Viaduct (see online version for colours)

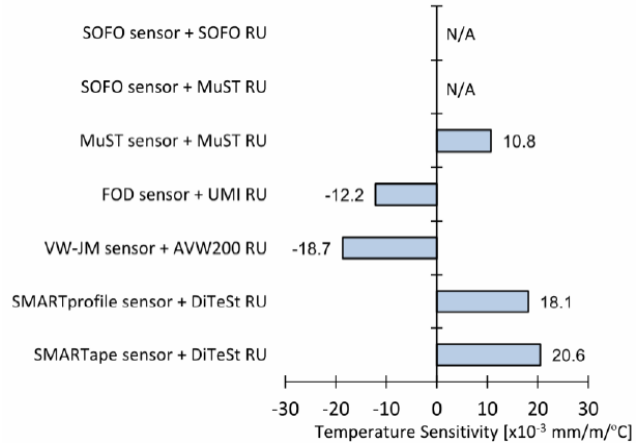

All other sensing systems exhibited non-negligible sensitivity to temperature variations. It means that a significant error can be present if no additional temperature compensation is made. It has to be noticed that by knowing the temperature influence on each sensor, it is possible to compensate the temperature effect on the sensors.

Despite the good results, the calculation of the temperature cross-sensitivity was performed based on data from field observations. It means that some other effects, always present in a real structure, can also influence these measurements. A reasonable agreement was achieved between the estimated sensitivities and those expected from theoretic sensitivities that are approximately 8.6 με/°C for the system based on FBG and 18 με/°C for Brillouin scattering. Concerning the solutions based on Fabry-Perot inteferometry and on a vibrating wire, they have been installed with extension rods to create the 1 m gauge length. The thermal expansion of these rods introduced cross-sensitivity of the long-gauge configuration to temperature variations. If needed, the thermal expansion coefficient of the rods material may be included in calculations, to extrapolate the cross-sensitivity to other gauge lengths.

A laboratory test, isolating the effects of the temperature would help to assess, in a more accurate approach, the effective sensitivity of the present systems. A more broad temperature range may be included in these tests. Even though, the reported results proved to be very helpful to understand the real effects of the temperature in real structural and environmental conditions.

5 On-site application

5.1 Monitoring of Ricciolo Viaduct

In order to illustrate the power of the use of the long-gauge sensors for SHM an on-site application is briefly presented in this section. The Ricciolo (‘curl’) viaduct is built in period 2004–2005 at the Lugano North exit of Swiss motorway A2. It consists of five spans with total length of 134 meters. The 35-metre long main span crosses Vedeggio torrential river. It is built in form of a curved box girder, post-tensioned in various directions. A view of the completed main span of the Ricciolo Viaduct is given in Figure 23.

Figure 23 View to main span of Ricciolo Viaduct (see online version for colours)

Figure 24 Sensors network for structural monitoring applied on Ricciolo Viaduct, (a) plan view (sensors not to scale) (b) position in the beam cross-section (see online version for colours)

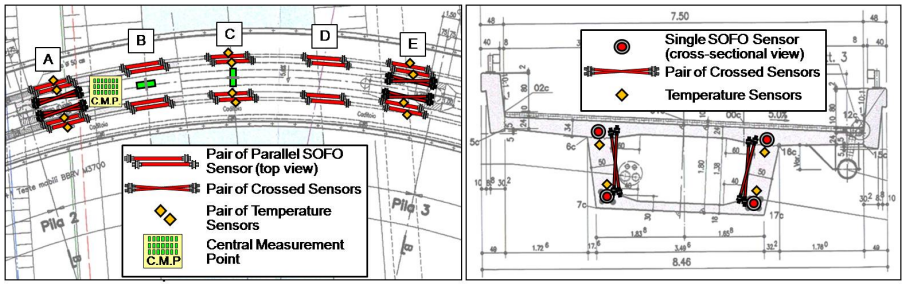

(a) (b)

The monitoring strategy for this curved pre-stressed bridge with fixed ends is presented in Figure 24. A long-gauge SOFO monitoring system was selected for this application. Sets of four long-gauge sensors combined in parallel topologies of were installed in five cross-sections of the main span of the bridge for monitoring axial strain, and bidirectional bending effects and corresponding curvatures assessment. Four pairs of sensors combined in crossed topologies were also installed on the lateral cross-section webs, near both extremities of the span, for assessment of the shear strains due to shear forces and torsion. Additionally, two inclinometers and 12 embedded thermo-couples were selected for tilt and torsion, and temperature appraisement, respectively. The long-gauge parallel sensors and associated thermo-couples were embedded in concrete during construction, while the crossed sensors and inclinometers were surface mounted (Glisic et al., 2008) after formwork removal.

Continuous monitoring started in January 2005, with one measurement session every hour, with the bridge still under construction and exposed to important works that might influence stress and stain distribution, including removal of formwork and post-tensioning. Beside the construction works, the structure was exposed to ambient temperature variations and concrete was subject to rheologic strain – creep and shrinkage.

5.2 Examples of data analysis

Detailed data analysis exceeds the topic of this paper, thus only results that highlight the potential of the developed long-gauge sensors based monitoring method are presented. More detailed analysis can be found in literature (Glisic et al., 2008). In order to illustrate the method, the characteristic cross-sections (cells) were analysed during the first four months and a half of monitoring. Bending effects and shear forces are presented on Figure 25. Diagram of vertical displacements, determined by double integration of curvature, is given in Figure 26. In both figures the changes in the structural behaviour during the construction works are clearly visible. The main works, such as,

1 the partial post-tensioning (30 to 70%) and partial lowering of formworks

2 the construction of the protection walls

3 the final post-tensioning (70 to 100%) and removal of external formworks are reliably detected (see Figure 25) (Glisic et al., 2008).

Figure 25 Results of the structural monitoring of Ricciolo Viaduct during the construction, (a) average curvatures in cells C and E (b) average shear strain due to vertical forces in cells A and E (see online version for colours)

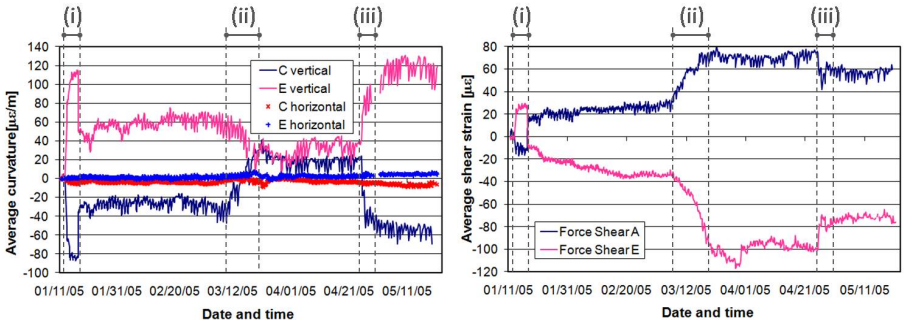

(a) (b)

Figure 26 Vertical displacements, (a) distribution of vertical displacements along elastic line during different stages of the construction works (b) distribution of horizontal displacements along elastic line during the same period (see online version for colours)

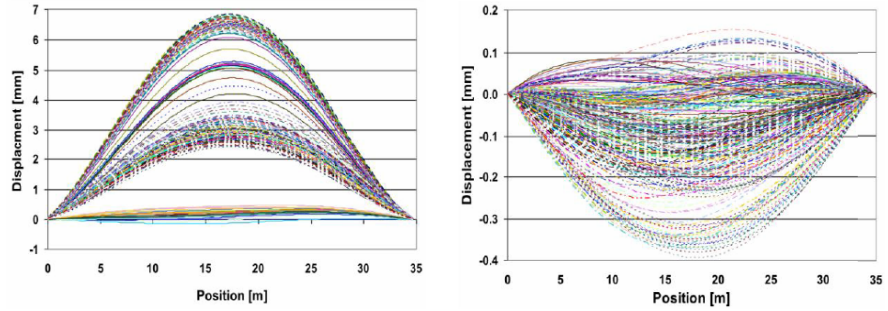

(a) (b)

6 Conclusions

The selection of the most suitable sensing system to apply in a particular SHM project is not simple and should be made taking into account the purpose of monitoring, the parameters to be monitored, the environment conditions in which the system will be installed, and the performance specifications of the available monitoring systems. This decision involves not only the knowledge of the structural system and its predictable behaviour, but also the familiarity with the measurement methods and the available sensing technologies and solutions.

SHM methods based on the use of long-gauge FOS have been developed and demonstrate a great potential for civil engineering applications. Besides the monitoring of

average strains, when combined with different topologies, this type of sensors allow for the monitoring of axial strain, curvature and shear strain, and for tracing diagrams of vertical and horizontal displacements.

A testing carried out both in controlled laboratory conditions and in uncontrolled on-site conditions gave indicators about the effective performance of six alternative fibre optic long-gauge solutions and one conventional solution based on vibrating wires. Four parameters were tested: accuracy of systems, precision of systems, temperature cross-sensitivity of the reading units, and temperature cross-sensitivity of the combined sensors and reading units. In general, all the solutions exhibited adequate characteristics for real in-field applications. However, if it is desired to achieve more accurate measurements it is necessary to improve the calibration procedures of the sensors and the temperature compensation procedures. The linear dependencies of the encoding parameters of both strain and temperature make the improvements of these procedures feasible and relatively simple. The selection of the most suitable technology to be applied to a specific project will therefore depend on the specific needs in terms of measurement accuracy, data acquisition frequency, gauge length, required number and density of sensors, environmental conditions (e.g., humidity, corrosion, electro-magnetic interferences), and budget. Table 2 summarises the main results of the tested solutions.

Table 2 Summary of the main results achieved during the assessment of long-gauge measurement systems

System	*A*	*B*	*C*	*D*	*E*	*F*	*G*
Sensor	SOFO	SOFO	MuST	FOD	VW-JM	SMART profile	SMART tape
Reading unit	SOFO VI	MuST Light	MuST Light	FTI 10	AVW 200	DiTeSt	DiTeSt
Slope error [%]	–1.6	–1.7	5.7	–0.4	4.9	2.7	–1.6
RMSE [με]	9.3	6.2	9.7	35.9	22.5	31.4	35.5
Repeatability [με]	1.4	0.2	0.5	0.6	0.0	13.9	N/A
Error range [με]	±2.1	±0.5	±0.9	±1.0	±0.1	±28.6	N/A
Temperature sensitivity RU – RMS [με]	2.6	0.2	0.6	2.0	N/A	18.9	N/A
Temperature sensitivity. Sensors – [με°C]	N/A	N/A	10.8	–12.2	–18.7	18.1	20.6

A structural monitoring strategy based on long-gauge sensors has been successfully applied on curved post-tensioned box girder of Ricciolo Viaduct in Switzerland. The main indicators concerning the structural behaviour, such as the bending and shear effects and the deformed shapes during the construction phase, were successfully monitored proving the efficiency of the method even in the case of highly inhomogeneous material such as post-tensioned reinforced concrete.

Acknowledgements

The authors would like to thank SMARTEC for the support, laboratory facilities and equipment that made this research possible. Carlos Rodrigues also thanks the FCT –

Portuguese Foundation for Science and Technology, and NewMensus for the financial support towards PhD programme SFRH/BDE/15645/2006.

References

Duplain, G., Belleville, C., Bussiere, S. and Belanger, P.A. (1997) 'Absolute fiber-optic linear position and displacement sensor', Paper presented at *Optical Fiber Sensors (OFS)*, 28 October 1997, Virginia, USA.

Glisic, B. and Inaudi, D. (2007) *Fiber Optic Methods for Structural Health Monitoring*, Wiley, Chichester.

Glisic, B., Posenato, D., Inaudi, D. and Figini, A. (2008) 'Structural health monitoring method for curved concrete bridge box girders', Paper presented at the *15th SPIE's Intl. Symp.*, 9–13 March 2008, San Diego, USA.

Horiguchi, T., Kurashima, T. and Tateda, M. (1989) 'Tensile strain dependence of Brillouin frequency shift in silica optical fibers', *IEEE Photonics Technology Letters*, Vol. 1, No. 5, pp.107–108.

Hornby, I.W. (1992) 'The vibrating wire strain gage', in Window, A.L. (Ed.): *Strain Gauge Technology*, 2nd ed., Elsevier Science Publishers, Ltd., Barking.

Inaudi, D. (1997) *Fiber Optic Sensor Network for the Monitoring of Civil Engineering Structures*, PhD thesis, Département de Génie Civil, Lausanne, École Polytechnique Fédérale de Lausanne, Switzerland.

Inaudi, D. (2000) 'Long-gage fiber-optic sensors for structural monitoring', in Rastogi, P.K. (Ed.): *Photomechanics, Topics in Applied Physics*, pp.273–293, Springer, Berlin.

Inaudi, D., Casanova, N., Kronenberg, P., Vurpillot, S. and Marazzi, S. (1997) 'Embedded and surface mounted fiber optic sensors for civil structural monitoring', *Proceedings of Smart Structures and Materials 1997*, SPIE, Vol. 3044, pp.236–243.

Inaudi, D., Posenato, D. and Glisic, B. (2005) 'Demodulating interferometric and FBG sensors in the spectral domain', *Proceedings of Smart Structures and Materials 2005*, SPIE, Vol. 5758, pp.70–75.

Kersey, A.D., Davis, M.A., Patrick, H.J., LeBlanc, M. and Koo, K.P. (1997) 'Fiber grating sensors', *Journal of Lightwave Technology*, Vol. 15, No. 8, pp.1442–1462.

Lienhart, W. (2005) 'Experimental investigation of the performance of the SOFO measurement system', *Proceedings of the 5th International Workshop on Structural Health Monitoring*, Stanford, USA, pp.1131–1138.

Measures, R.M. (2001) *Structural Monitoring with Fiber Optic Technology*, Academic, London.

Nikles, M., Thevenaz, L. and Robert, P.A. (1996) 'Simple distributed fiber sensor based on Brillouin gain spectrum analysis', *Optics Letters*, Vol. 21, No. 10, pp.758–760.

Othonos, A. (1997) 'Fiber Bragg gratings', *Review of Scientific Instruments*, Vol. 68, No. 12, pp.4309–4341.

Petuchowski, S., Giallorenzi, T. and Sheem, S. (1981) 'A sensitive fiberoptic Fabry-Perot-interferometer', *IEEE Journal of Quantum Electronics*, Vol. 17, No. 11, pp. 2168-2170.

Ravet, F., Briffod, F., Glisic, B., Nikles, M. and Inaudi, D. (2009) 'Submillimeter crack detection with Brillouin-based fiber-optic sensors', *IEEE Sensors Journal*, Vol. 9, No. 11, pp.1391–1396.

SHMII (2009) *Proceedings of ISHMII-4, The 4th International Conference on Structural Health Monitoring of Intelligent Infrastructure, Conference CD*, Zurich, Switzerland.

Thevenaz, L., Facchini, M., Fellay, A., Robert, P., Inaudi, D. and Dardel, B. (1999) 'Monitoring of large structure using distributed Brillouin fiber sensing', *Proceedings of 13th International Conference on Optical Fiber Sensors*, Kyongju, Korea, SPIE, Vol. 3746, pp.345–348.

Yoshino, T., Kurosawa, K., Itoh, K. and Ose, T. (1982) 'Fiber-optic Fabry-Perot interferometer and its sensor applications', *IEEE Journal of Quantum Electronics*, Vol. 18, No. 10, pp.1624–1633.